An elaborate low-temperature electrolyte design towards high-performance liquid metal battery

Reference:
H. Xie; Z. Chen; P. Chu, et al., An elaborate low-temperature electrolyte design towards high-performance liquid metal battery. Journal of Power Sources 2022, 536, 231527.

ISSN 0378-7753 (2022), Copyright © 2022 Elsevier B.V. All rights reserved
Full text (Publisher's DOI): https://doi.org/10.1016/j.jpowsour.2022.231527
Received 23 December 2021, Revised 11 April 2022, Accepted 22 April 2022, Available online 29 April 2022, Version of Record 29 April 2022

An elaborate low-temperature electrolyte design towards high-performance liquid metal battery

Hongliang Xie[a], Zhiyuan Chen[c], Peng Chu[a], Jie Wang[a], Zehao Li[a], Hailei Zhao[a,b,1*]

[a] School of Materials Science and Engineering, University of Science and Technology Beijing, Beijing, 100083, China
[b] Beijing Municipal Key Lab for Advanced Energy Materials and Technologies, Beijing, 100083, China
[c] Separation and Conversion Technology, Flemish Institute for Technological Research, 2400 Mol, Belgium

Abstract: Liquid metal battery (LMB) with low cost, excellent cycle performance and flexible scalability is developed as a promising solution for large-scale energy storage. However, the high melting point of the electrolyte necessitates an elevated operating temperature, which provokes aggravated hermetic seal and corrosion issues, seriously inhibiting the advancement of LMBs. Herein, we elaborately design a novel LiCl-LiBr-KBr electrolyte system based on the mass triangle model to overcome this obstacle. The LiCl and LiBr components can provide required lithium ionic conduction, while the KBr plays a dual role of decreasing the melting point and suppressing metal lithium dissolution. The designed LiCl-LiBr-KBr (33:29:38 mol%) electrolyte possesses low melting point (T_m=327 ^oC), and high ionic conductivity (1.573 S cm^{-1} at 420 ^oC), which enables the Li||Bi battery to work efficiently at 420 ^oC with high energy efficiency (83%), excellent rate capability, superior cycling stability and freeze/thaw performance. This represents an 80-130 ^oC decrease in operating temperature compared to most reported LMBs. The unique performance combination together with its low cost makes the designed electrolyte extremely attractive for low-temperature LMB.

[1*] Corresponding author: H. Zhao, email: hlzhao@ustb.edu.cn, hlzhao66@outlook.com; Tel: +86-10-82376837; Fax: +86-10-82376837.

Keywords: Energy storage; Liquid metal battery; Molten salt; Electrolyte; Electrochemical performance

1. Introduction

The exploitation and utilization of renewable energy sources, such as wind and solar, are expected to be pursued extensively in the coming years for coping with the energy crisis and environmental degradation effectively [1-4]. However, owing to the intrinsic intermittence and fluctuation, the electricity generated from renewable energy sources needs to be first saved in energy storage systems before being incorporated into the power grid to maintain the grid reliability and stability and increase the efficiency of power transmission and distribution [5-9]. As a potential candidate for large-scale energy storage technology, liquid metal battery (LMB), proposed by Sadoway et al. in 2006, has drawn growing attention because it holds promise to meet the requirements of energy storage for smart grid in terms of energy density, service life and material cost [10-13].

A typical LMB is composed of liquid metal positive and negative electrodes, and molten salt electrolyte. Different from the solid-liquid electrode-electrolyte interface of lithium-ion battery, its unique liquid/liquid electrode/electrolyte interface facilitates the mass and charge transfer during operation. Combined with the high ionic conductivity (>1 S cm^{-1}, two orders of magnitude higher than that of lithium-ion battery electrolyte [13-15], the accelerated electrode reaction kinetics and excellent rate performance of the LMB can be expected. Its all-liquid battery construction circumvents the electrode microstructure degradation that generally occurs in the lithium-ion battery and so grants LMBs the potential for ultralong service life. During the LMB fabrication, the electrode and electrolyte generally adopt metal/alloy and metal halide salts, without any binder, conductive additive, or separator inclusion during cell fabrication, enabling a low raw material and assembly cost. Furthermore, ascribed to the water-soluble

feature of the salt electrolyte, it can be removed by water-washing and consequent simple treatment for recycle without environment pollution. Both positive and negative electrodes are metal or alloy, they can be reused directly without the requirements of dismantling, metals leaching, and separation for valuable elements recycling. This superiority renders it more competitive in battery recycling, which is a major dilemma for the lithium-ion battery market.

Lithium represents the most promising negative electrode due to its desirable properties of low melting point (180.5 ^{o}C), lowest negative electrochemical potential (-3.04 V versus standard hydrogen electrode), and high specific capacity (3860 mAh g^{-1}) [16,17]. In recent years, extensive efforts have been devoted to developing high-performance Li-based LMBs for large-scale energy storage. Molten salt electrolyte, as an essential component of LMB, plays a dual role of conducting lithium ions and separating negative and positive electrodes. It can be the determinant factor of operating temperature, rate performance, Coulombic and energy efficiencies of LMB. Note that energy efficiency refers to the ratio of discharge energy to charge energy of the battery. With the extensive research on Li-based LMBs, several electrolyte systems have been proposed and applied successfully [18-23]. The LiF-LiCl-LiBr (22:31:47 mol%, T_m=430 ^{o}C) electrolyte has been widely used in Li||Sb-Sn [18], Li||Te-Sn [19], and Li||Bi-Ga [20] batteries. Its super-high ionic conductivity (above 3.21 S cm^{-1}) enables these batteries to deliver high energy efficiency and excellent rate performance at 500 ^{o}C. The LiF-LiCl (30:70 mol%, T_m=501 ^{o}C) electrolyte is applied to the Li||Bi battery, which presents a good cycle stability and a high Coulombic efficiency of 99% at 550 ^{o}C [21]. However, these electrolytes are featured by high melting point, which compulsively requires the batteries to work at high temperatures (500-550 ^{o}C). High operation temperature raises the potential concerns of LMBs about long-term hermetic seal, battery components corrosion, maintenance costs and safety issues.

To circumvent the above issues, decreasing the melting point of molten salt electrolyte

becomes extremely imperative. In this context, the low-melting-point electrolyte systems LiCl-LiI (36:64 mol%, T_m=368 ^oC) and LiI-KI (58:42 mol%, T_m=260 ^oC) were proposed by Song and Lu groups [22,23], with which the batteries could work at temperatures as low as 410 and 290 ^oC, respectively. Nevertheless, the Li|LiI-KI|Bi-Sn cell displays a very large polarization when operating at 290 ^oC [23], which leads to a low discharge voltage and a significantly decreased charge/discharge energy efficiency. Excessively low operating temperature causes a reduced lithium ion diffusivity in both electrolyte and electrode, and therefore incurs sluggish electrode reaction kinetics. Simply pursuing low operating temperature by designing electrolyte with low melting points is not advisable from the viewpoint of the overall performance of LMB. Especially, the reported low-melting-point electrolyte always includes LiI, while its high price may limit the commercial application of the related LMB for large-scale energy storage. Therefore, it remains a great challenge for applicable electrolyte design. To couple with current mature electrode materials, a cost-effective electrolyte with high conductivity and moderate melting point is strongly desired, which is expected to break the dilemma of LMB technology between long-term operating stability and electrochemical performance as well as material cost.

LiCl-LiBr-KBr ternary molten salt possesses low melt point (310 ^oC at 25:37:38 mol%) and considerable ionic conductivity (ca. 1.36 S cm^{-1} at 425 ^oC), which is used in Li-alloy/metal disulfide batteries [24-27]. The Li-Al|LiCl-LiBr-KBr|FeS_2 system could operate at 398 ^oC with excellent long cycle stability (80% of initial capacity after 1000 cycles) [28]. To realize better battery performance, some efforts have been devoted to improving the LiCl-LiBr-KBr electrolyte, such as composition optimization and additive incorporation. The modified composition (34:32.5:33.5 mol%) achieves a 25% improvement of conductivity to 1.7 S cm^{-1} at 425 ^oC but is accompanied by an undesirable large increase in melting point (50 ^oC) [27]. No more optimized composition has been reported so far. To obtain a composition with low

melting point and meanwhile high conductivity, and so realize its use in LMB, further exploration is imperative.

In this work, a novel electrolyte composition (LiCl-LiBr-KBr=33:29:38 mol%) is elaborately designed based on the consideration of melting point and ionic conductivity with the help of mass triangle model calculation. The LiCl and LiBr salts offer fast lithium ionic conduction for electrolyte, while KBr, as an elaborate component, can significantly reduce the melting point of the electrolyte thermodynamically, enabling a low operating temperature for Li-based LMBs. Additionally, considering the fact that the metal lithium solubility could be decreased by using multiple cations in molten salt [12,29], the KBr addition can help to mitigate the self-discharge phenomenon of battery, thus affording a high Coulombic efficiency. The synergetic effect of these advantages enables the prepared LMB with the designed LiCl-LiBr-KBr electrolyte to show a unique combination of low operating temperature and outstanding electrochemical performance. The constructed Li|LiCl-LiBr-KBr|Bi battery can efficiently work at 420 ^{o}C with impressive voltage efficiency (86.2%, the ratio of discharge midpoint voltage to charge midpoint voltage) and high Coulombic efficiency (>97%) at 100 mA cm^{-2}, and deliver excellent rate-capability with no obvious capacity degradation when the current density increases from 100 to 400 mA cm^{-2} as well as outstanding long-term cycling stability. Combined with the low material cost (219.75 \$ kg^{-1}), the designed LiCl-LiBr-KBr electrolyte not only delivers great prospects for extensive applications, but also provides a pathway towards the development of innovative low-temperature LMBs for grid-scale energy storage.

2. Experimental section

2.1. Pretreatment of electrolyte

High purity (> 99%) and anhydrous raw materials of LiCl, LiBr, and KBr from Shanghai Aladdin Biochemical Technology Co., Ltd. were used to prepare the molten salt electrolyte. The appropriate stoichiometry of the raw materials was weighed and mixed evenly, then

transferred to an alumina crucible in a glove box with a high-purity Ar atmosphere (O_2 < 0.1 ppm, H_2O < 0.1 ppm). To get homogeneous and anhydrous molten salt electrolytes, the salt mixtures were heated at 150 °C for 20 h and then 290 °C for 40 h in a vacuum to remove residual water. Subsequently, they were melted at 550 °C for 6 h under an Ar atmosphere.

2.3. Characterization of electrolyte

The melting point of the electrolyte was analyzed by the differential scanning calorimetry (DSC, TADSC25, USA) with a heating rate of 20 °C min^{-1}. Cyclic voltammetry (CV) test was used to examine the electrochemical stability of the electrolyte in -0.5-1.5 V electrochemical window by frequency response analyzer (Solartron 1260A, England) combined with a Solartron 1287 electrochemical interface. The phase identification of the designed electrolyte was conducted by X-ray diffraction (XRD, Rigaku D/max-A, Cu-Kα radiation, λ=1.5406 Å, Japan).

2.4. Fabrication of prototype battery

The prototype battery (Figure S1) was assembled at a fully charged state in a glove box under an Ar atmosphere to circumvent the adverse effect of water and oxygen on the active components inside the battery. Pure Li (99.9%, Aladdin), absorbed in Ni-Fe foam (negative current collector), was used as negative electrode. Pure Bi (99.994%, Trillion Metals) was, as positive electrode, pre-melted in graphite crucible for 2 h at 350 °C. The obtained Bi positive electrode was first placed at the bottom of the container, and then the required amount of molten salt electrolyte was added. The container was then heated at 550 °C for 3 h to fully melt the positive electrode and electrolyte again. Subsequently, the prepared negative electrode was inserted into the melted electrolyte, maintaining a distance of ca. 16 mm from the positive electrode. Finally, the battery was sealed when cooled down to room temperature. The mass of each material involved in Li|LiCl-LiBr-KBr|Bi cell with a theoretical capacity of 500 mAh is listed in Table S1. After assembly, the battery was heated in a vertical tube furnace at a rate of

10 ^{o}C min^{-1}, and held at designed operating temperature for 3 h before data collection.

2.5. Battery performance Measurements

Galvanostatic charge/discharge tests in a voltage range of 0.1-1.5 V were performed on a battery testing device (LAND, CT2001A, China). The self-discharge current was measured by the stepped-potential method. Since the open-circuit voltage of the Li||Bi LMB is 0.86-0.77 V [12], a voltage of 1.0 V was applied at the first stage and 1.2 V at the second stage. During the potential step charging, the current dropped down to a constant low value, which corresponds to the self-discharge current. Post-mortem analysis was carried out to check the inside microstructure of cycled battery and so evaluate the suitability of electrolyte density. The batteries discharged to a target depth was cooled down to room temperature, opened and sectioned in Ar-filled glove box. The microstructure and element distribution at positive electrode/electrolyte interface were observed by scanning electron microscopy (SEM, Zeiss Supra 55, 10 kV accelerating voltage, Germany) equipped with energy dispersive spectrometer (EDS). The freezing and thawing measurement was performed on the battery to illustrate the effect of large temperature fluctuations on battery performance. The test was carried out by cooling the battery down to room temperature, and then rising to operating temperature and restarting the battery test procedure.

3. Results and discussion

3.1. LiCl-LiBr-KBr electrolyte design

To effectively alleviate the high-temperature operation issues and further improve the application prospect of Li-based LMBs, a LiCl-LiBr-KBr ternary molten salt electrolyte system was designed. The melting point and ionic conductivity of the electrolyte play the dominant roles in operating temperature and electrochemical performance of the battery. Therefore, first, the mass triangle model was employed to predict the melting point and ionic conductivity of the LiCl-LiBr-KBr system based on the reported corresponding data [27,30,31]. The calculated

melting point diagram is displayed in Figure 1a. When the molar ratio of LiCl, LiBr, and KBr is 25:37:38 mol% (marked as point *a*), the LiCl-LiBr-KBr system registers a low eutectic point of 310 °C, which is much lower than that of other widely used electrolytes in LMBs [18-20]. Just at 400 °C, the LiCl-LiBr-KBr system can provide a wide liquid phase range. It can be anticipated that, if the LiCl-LiBr-KBr salt is adopted as electrolyte, the operating temperature of LMBs could be greatly reduced.

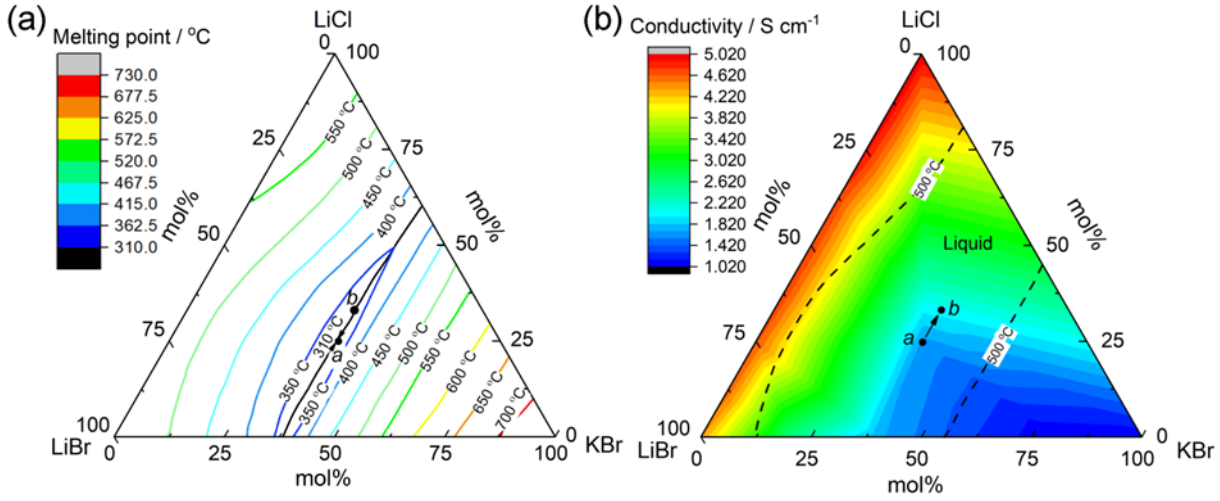

Figure 1. Calculated phase diagram (a) and ionic conductivity at 500 °C (b) of LiCl-LiBr-KBr ternary system.

Further, the isothermal conductivities of LiCl-LiBr-KBr system are calculated and the results are depicted in Figure 1b. Two 500 °C isotherms are plotted, with liquid phase in between and solid phase on both sides. To be noted, during the calculation process, the predicted ionic conductivities of the LiCl-LiBr-KBr ternary compositions, where the stable phases are solids, were considered to be the values of the corresponding pseudo liquid phase obtained by supercooling. It can be broadly defined as three areas for the conductivity: blue color represents the low conductivity area with 1-2 S cm^{-1}, green color represents the medium conductivity area with 2-4 S cm^{-1}, and orange color indicates the high conductivity area with 4-5 S cm^{-1}. The eutectic composition (point *a*) is located in the low conductivity area, which is

not desired because low ionic conductivity of electrolyte will limit the ion transport and cause large internal resistance, leading to poor rate performance and low energy efficiency of the battery. Therefore, we have to make a trade-off between system melting point and ionic conductivity.

Based on the consideration of improving the ionic conductivity while controlling the increase of melting point as much as possible, we optimize the composition of the LiCl-LiBr-KBr system by moving the eutectic point *a* to *b* along the lower temperature black line, as indicated in Figure 1a. Point *b* (33:29:38 mol%) is capable of delivering a moderate melting temperature of 327 ^{o}C, which is confirmed by the DSC measurement (Figure S2). Although the melting temperature of point *b* is slightly higher than that of the low eutectic point, it is still acceptable since this temperature is still much lower than that of most LMB electrolytes [20-22]. More strikingly, this elaborate composition (33:29:38 mol%) lies at the boundary of medium and low conductivity areas and so attains a higher ionic conductivity of 2.03 S cm^{-1}, meaning a 23% increase compared to that of the low eutectic point, which is a quite good conductivity level. The designed LiCl-LiBr-KBr salt (33:29:38 mol%) is expected to present excellent performance as electrolyte for low-temperature LMBs.

3.2. Operating temperature optimization of Li|LiCl-LiBr-KBr|Bi battery

Encouraged by the low melting point and desirable ionic conductivity, the LiCl-LiBr-KBr salt (33:29:38 mol%) was adopted as the electrolyte for the prototype LMBs to analyze the electrochemical properties at different temperatures. Note that the LiCl-LiBr-KBr salt (33:29:38 mol%) is abbreviated as LiCl-LiBr-KBr in the following for the convenience of description. During the fabrication process, Li and Bi were designed as negative and positive electrodes, respectively. This is because their melting temperatures (180 ^{o}C for Li, and 271.3 ^{o}C for Bi) are much lower than that of LiCl-LiBr-KBr electrolyte, and therefore do not constitute the restricted factor for battery operating temperature. As shown in Figure 2a, the

Li|LiCl-LiBr-KBr|Bi cell cycles stably at 100 mA cm^{-2} at 500 ^{o}C, indicating the feasibility of LiCl-LiBr-KBr electrolyte application in LMBs. Meanwhile, it is also worth mentioning that the discharge voltage profile of this cell can be divided into two regions according to the different reaction processes. In Region I, the voltage decreases gradually, which represents the formation of a homogeneous Li_xBi liquid phase at the initial stage of discharge. In the subsequent Region II, the solid product Li_3Bi is continuously generated and coexists with Li_xBi liquid phase, leading to a constant discharge voltage, which conforms to the discharge process of the reported Bi-based cathode materials [20,21]. These results demonstrate that the battery charge-discharge mechanism is not changed with LiCl-LiBr-KBr electrolyte employed.

When the operating temperature decreases to 380 ^{o}C, the Li|LiCl-LiBr-KBr|Bi cell could still operate with an excellent electrochemical performance at 100 mA cm^{-2}. As shown in Figure 2b, at 380 ^{o}C, this cell delivers a high discharge voltage of 0.69 V as that at 500 ^{o}C. Impressively, much high Coulombic and energy efficiencies of 98.8% and 80.9% can be realized at 380 ^{o}C, respectively. The low working temperature of 380 ^{o}C, which is at least 25% lower than that of the current LMBs, together with the attractive battery performance at this temperature, demonstrates the promising of the designed LiCl-LiBr-KBr salt as electrolyte for low-temperature LMBs.

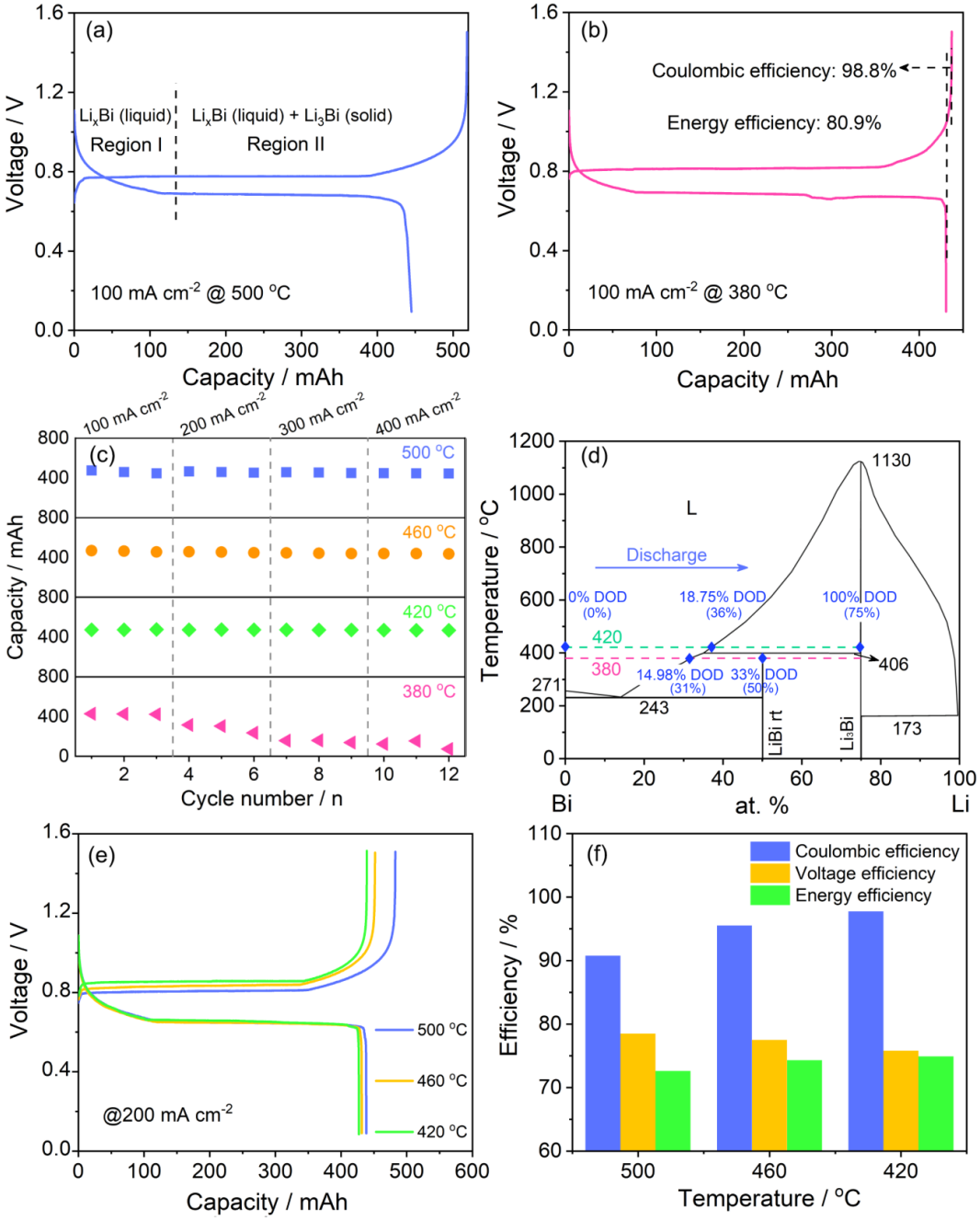

Figure 2. Li|LiCl-LiBr-KBr|Bi battery: Charge and discharge voltage curves at 100 mA cm^{-2} at 500 °C (a) and 380 °C (b); Temperature influence of discharge capacity at different current densities of Li|LiCl-LiBr-KBr|Bi from 500 to 380 °C (c). Li-Bi binary phase diagram (obtained from https://materials.springer.com). The values in the brackets under different depths of discharge (DODs) represent the mole percentage of lithium in the positive electrode (d). Voltage-capacity curves (e) and derived Coulombic, voltage and energy efficiencies (f) at 200 mA cm^{-2} at 500, 460 and 420 °C.

To optimize the operating temperature, the cycling performance of the Li|LiCl-LiBr-KBr|Bi cell was examined at different temperatures from 500 to 380 ^{o}C. As depicted in Figure 2c, when the temperature is above 420 ^{o}C, the Li|LiCl-LiBr-KBr|Bi cell exhibits negligible capacity fade as the current density increases from 100 to 400 mA cm^{-2} and less influence of temperature on the capacity delivery. While, at 380 ^{o}C, significant performance degradation can be observed when reaching 200 mA cm^{-2}. At 400 mA cm^{-2}, the battery performance decays seriously with much low capacity remained and much large voltage polarization (Figure S3). The electrochemical performance demonstration of cell is strongly related to the phase evolution of electrode materials during charge/discharge process. Based on the Li-Bi binary diagram as presented in Figure 2d, at 420 ^{o}C, as the discharge electrode reaction proceeds, the lithium content in the positive electrode Bi increases continuously, and the positive electrode (Bi-Li) exists in the liquid state in the initial discharge stage. When the Li mole fraction increases to 36%, corresponding to 18.75% DOD (detailed calculation see page 4 in Supporting Information), the Li_3Bi solid phase starts to generate, and the positive electrode moves to the solid-liquid two-phase zone (Li_3Bi + Li (36 mol%)-Bi liquid). Before discharge process is fully completed, the two phases will be kept and just their weight ratio changes upon discharging, the content of Li_3Bi increases progressively. The coexisting liquid phase helps to accelerate the electrode reaction, thereby ensures an excellent electrochemical performance even at high current density. The cases at 460 and 500 ^{o}C are similar to that at 420 ^{o}C, but the single liquid phase region is extended.

However, if the operating temperature is lowered to 380 ^{o}C, as noted by the pink line in Figure 2d, not only does the positive electrode advance into the two-phase zone (31 mol% of Li content, 14.98% DOD), but the phase evolution is much different from that at 420 ^{o}C. Since the melting point of the LiBi phase is 406 ^{o}C, discharging at 380 ^{o}C, the LiBi solid phase will be first formed when Li content reaches 31 mol%, and two phases of Bi-rich Li-Bi liquid and

LiBi solid will coexist until the point of 50 mol% Li (33% DOD). After that, further discharge makes the system enter two-solid-phase area, LiBi + Li_3Bi, which will be maintained until the end of the discharge. The all-solid electrode state results in a low Li diffusion rate and so sluggish electrode reaction kinetics, explaining the poor electrochemical performance at a higher current density at 380 ^oC. Therefore, it is concluded that 380 ^oC is not a desirable choice for battery operation of Li|LiCl-LiBr-KBr|Bi system.

The voltage-capacity curves of the Li|LiCl-LiBr-KBr|Bi cell at different temperatures show that the operating temperature has somewhat influence on the charge voltage while negligible effect on the discharge voltage (Figure 2e). The polarization voltage increases slightly with decreasing temperature. More importantly, when the temperature decreases from 500 to 420 ^oC, only slight capacity degradation can be observed, indicating the good electrode reaction kinetics at 420 ^oC. Meanwhile, as shown in Figure 2f, this cell exhibits a high Coulombic efficiency of 98.23% at 420 ^oC, meaning a 9% improvement compared to that at 500 ^oC. Moreover, a high energy efficiency of 74.9% can also be achieved under this operating condition, even higher than that of 500 ^oC (72.6%). These results demonstrate that 420 ^oC is the preferable operating temperature for the Li|LiCl-LiBr-KBr|Bi cell.

The subsequent calculation of isothermal conductivity reveals that the designed LiCl-LiBr-KBr electrolyte presents also a high ionic conductivity of 1.573 S cm^{-1} at 420 ^oC (Figure S4).

3.3. Low-temperature electrochemical performance of Li|LiCl-LiBr-KBr|Bi battery

The various electrochemical performance of the Li|LiCl-LiBr-KBr|Bi cell operating at 420 ^oC was investigated. As shown in Figure 3a, the Li||Bi cell with the designed electrolyte offers an outstanding discharge voltage of 0.692 V at 100 mA cm^{-2} with only 0.028 V of negligible overvoltage observed compared to the Li||Bi electromotive force (0.72 V) [32]. Even at a high current density of 400 mA cm^{-2}, this cell exhibits still a high discharge voltage of 0.543 V, suggesting its superior rate performance than other low-temperature Li-based LMBs [22,23].

Of course, the Li|LiCl-LiBr-KBr|Bi cell could work at even higher current density when the operating temperature increases to 460 or 500 °C (Figure S5 and S6) because of the more superior ionic conductivity of LiCl-LiBr-KBr electrolyte at high temperature.

Meanwhile, this cell attains high and stable Coulombic efficiencies (Figure 3b), greater than 97% at the current densities of 100-400 mA cm^{-2}, especially 99.4% at 400 mA cm^{-2}, which significantly surpasses that of Li|LiF-LiCl-LiI|Sb-Pb [33], Li|LiF-LiCl|Sb-Bi [34], and Li|LiF-LiCl-LiBr|Sn systems [35], manifesting the high electrochemical reversibility. As for energy efficiency, this cell reaches an impressive value of 83.0% at 100 mA cm^{-2}. Even at 400 mA cm^{-2}, about 56.0% of energy efficiency can be retained, which is much higher than that of low-temperature system Li|LiCl-LiI|Bi-Pb [22]. These results demonstrate the superiority of the designed molten salt electrolyte used for high efficiency LMBs.

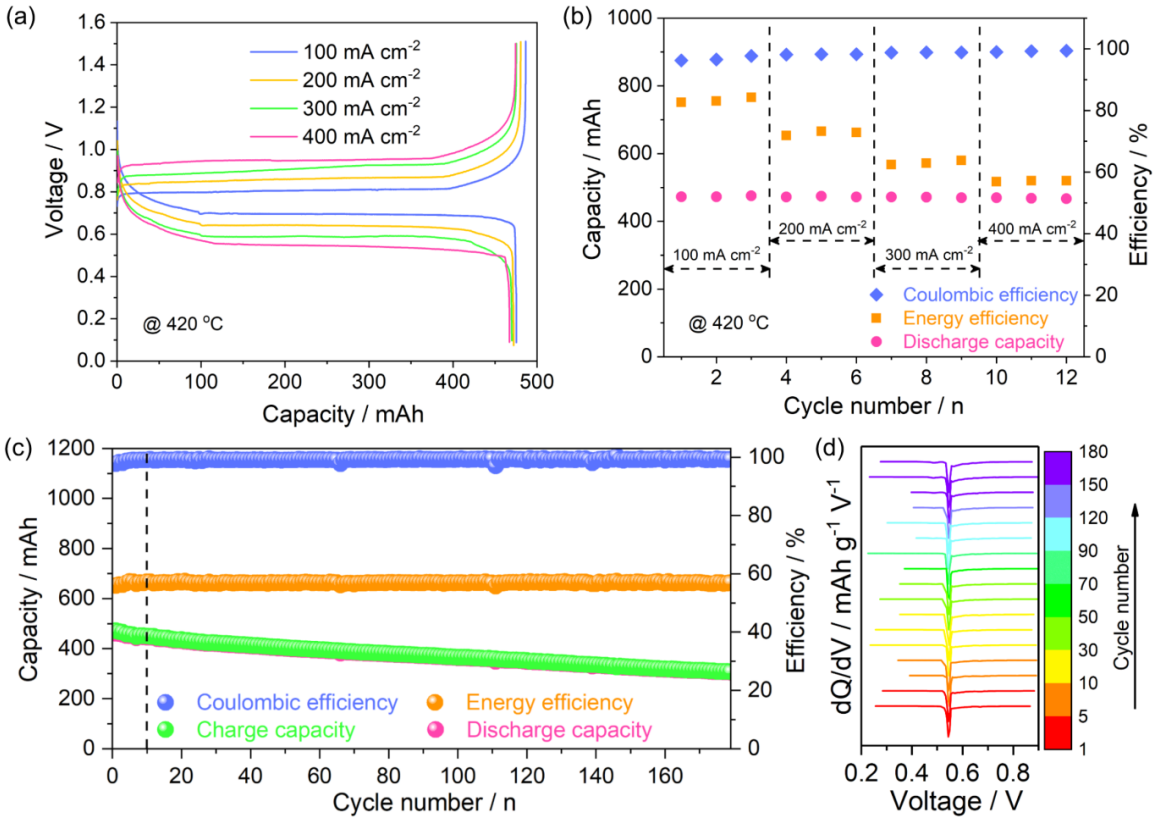

Figure 3. Charge and discharge voltage curves (a) and detailed Coulombic and energy efficiencies, and discharge capacity versus cycle number (b) at different current densities (from 100 to 400 mA cm^{-2}) of Li|LiCl-LiBr-KBr|Bi at 420 °C. (c) Long cycle performance of Li|LiCl-

LiBr-KBr|Bi cell tested at 400 mA cm^{-2}. (d) Differential capacity curves of Li|LiCl-LiBr-KBr|Bi cell during lithiation process at 400 mA cm^{-2}.

We conducted the comparison of our designed electrolyte with the reported composition of LiCl-LiBr-KBr (34:32.5:33.5 mol%) salt, which was used for LiAl/FeS_2 battery [27]. The results (Figure S7) show that the battery with the designed electrolyte (LiCl:LiBr:KBr=33:29:38 mol%) delivers much lower polarization voltage at different current densities at 420 ^oC, further indicating the meliority of the designed electrolyte and the corresponding methodology.

The cyclability of the Li|LiCl-LiBr-KBr|Bi cell was studied at 420 ^oC. As shown in Figure 3c, this cell exhibits stable long-cycle performance over 170 charge and discharge cycles. There is almost no difference in the charge and discharge capacities of each cycle during the whole test, corresponding to a high Coulombic efficiency over 99%, suggesting an ignorable self-discharge current and stable electrochemical operation state of the battery. It should be noted that the slow increase of the Coulombic and energy efficiencies in the initial 10 cycles is ascribed to the gradual improvement of wettability between lithium negative electrode and Ni-Fe foam current collector [16]. The waterfall type differential capacity (dQ/dV) curves of battery at different cycles during lithiation and delithiation processes are shown in Figure 3d and S8, respectively. The related color map is also attached to clearly show the position of each peak in the dQ/dV curves. The peaks for the lithiation and delithiation processes are at about 0.54 V and 0.965 V, respectively, with negligible variation during long-term cycling, indicating the high reversibility of electrode reaction, which should be responsible for the high and constant energy efficiency (Figure 3c). Additionally, the change of charge and discharge midpoint voltages (Figure S9) is also negligible, conforming to the differential capacity result. These results demonstrate that the battery performance of Li|LiCl-LiBr-KBr|Bi system at 420 ^oC outperforms most of the previous LMB works in terms of operating temperature,

reversibility, and cycling stability, representing a significant step towards the practical realization of low-temperature LMBs with excellent electrochemical performance.

3.4. Properties of LiCl-LiBr-KBr electrolyte

The superior electrochemical performance of Li|LiCl-LiBr-KBr|Bi cell at low temperature (420 ^{o}C) is inseparable from the intrinsic properties of the designed electrolyte. Self-segregating characteristic is critical for LMBs, which requires the density of electrolyte to be intermediate to that of electrode materials. The density of LiCl-LiBr-KBr salt was estimated based on weighted average calculation of constituents, assuming no volume effect occurs with temperature (Equation S3 and Table S2) [12]. The material densities of the calculated electrolyte, employed electrodes (Li and Bi), as well as the discharge product are listed in Table 1 [21]. Obviously, the density of LiCl-LiBr-KBr salt (2.08 g cm^{-3}) is validated to be appropriate, lying between that of Li (negative electrode) and Bi (positive electrode). Even if the intermetallic compound (Li_3Bi, 5.06 g cm^{-3} in Table 1) is formed at the positive electrode side as electrode reaction proceeds, the designed electrolyte could also locate above the whole positive electrode, keeping the two electrodes separated.

Table 1. Densities of electrode materials, discharge product and the designed electrolyte.

Material	Li	LiCl-LiBr-KBr	Li_3Bi	Bi
Density / g cm^{-3}	0.51	2.08	5.06	10.05

To demonstrate this point directly, the cross-section of the positive electrode at 40% DOD after 5 cycles was characterized by SEM. For the SEM sample preparation, when the battery reached the target cycle state (40% DOD), the test program and temperature control system were stopped to cool the battery down to room temperature. The cooled battery was then opened and sectioned in a glove box under Ar atmosphere. As shown in Figure S10 and 4a, it

is revealed that the electrolyte locates above the positive electrode, and there is a distinct boundary between them. It is noteworthy that the lithium element cannot be detected directly by the EDS technique due to the low atomic number. However, the dissected section is inevitably exposed to air when transferred from the holder to the SEM chamber. The easy oxidization feature of lithium allows its distribution to be reflected by the oxygen element. As shown in Figure 4b-d, the existence of O and Bi elements in the middle layer represents the discharge product of Li_3Bi of positive electrode, while the bright Bi layer at the bottom layer corresponds to the unreacted positive electrode Bi. The presence of Br element in the upper layer indicates the distribution of the LiCl-LiBr-KBr electrolyte, which further proves the suitable density of designed electrolyte in the whole charge-discharge process.

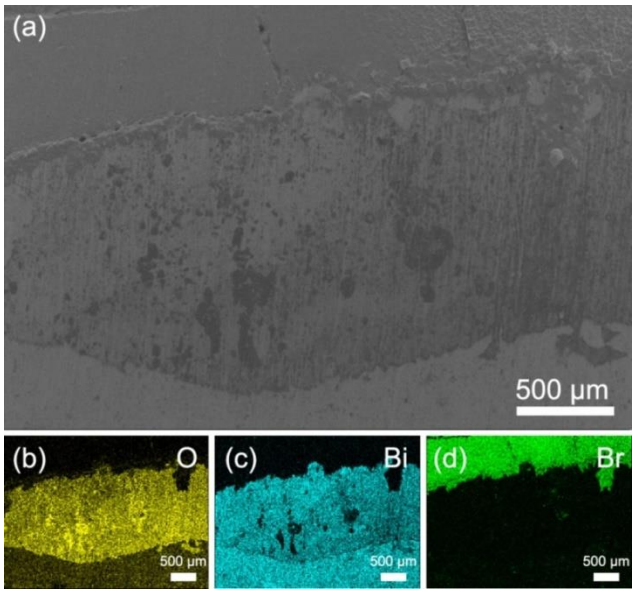

Figure 4. SEM image of cross-section (a) and EDS element mapping images (b, c, d) of the positive electrode at 40% DOD after 5 cycles.

To understand the chemical and electrochemical stability of the designed electrolyte with Bi positive electrode, the thermodynamic calculations were performed for the decomposition of molten salts and for their possible reactions with Bi cathode. All the reactions show large positive Gibbs free energies (Figure S11), suggesting the chemical stability of the LiCl-LiBr-

KBr electrolyte applied in Li||Bi battery. The electrolysis potentials of these possible reactions at different temperatures (300-500 ^{o}C) derived based on Nernst equation are shown in Figure 5a. All the considered reactions exhibit decomposition potentials vs. Li/Li^{+} greater than 2.5 V, which is much higher than the working voltage range of the LMBs (< 2.0 V) [20,21], manifesting the electrochemical stability of the LiCl-LiBr-KBr electrolyte in Li||Bi battery. Meanwhile, a Li|LiCl-LiBr-KBr|Li symmetrical cell was constructed for CV test in the potential range of -0.5-1.5 V vs. Li/Li^{+}. As shown in Figure 5b, only one pair of peaks is observed. The reduction peak potential at about -0.08 V corresponds to the lithium deposition process on the working electrode while the oxidation peak at about 0.09 V stems from the lithium stripping. No redundant peaks are observed in the CV curve, indicating again the stability of the LiCl-LiBr-KBr electrolyte in an electrochemical window of -0.5-1.5 V vs. Li/Li^{+}.

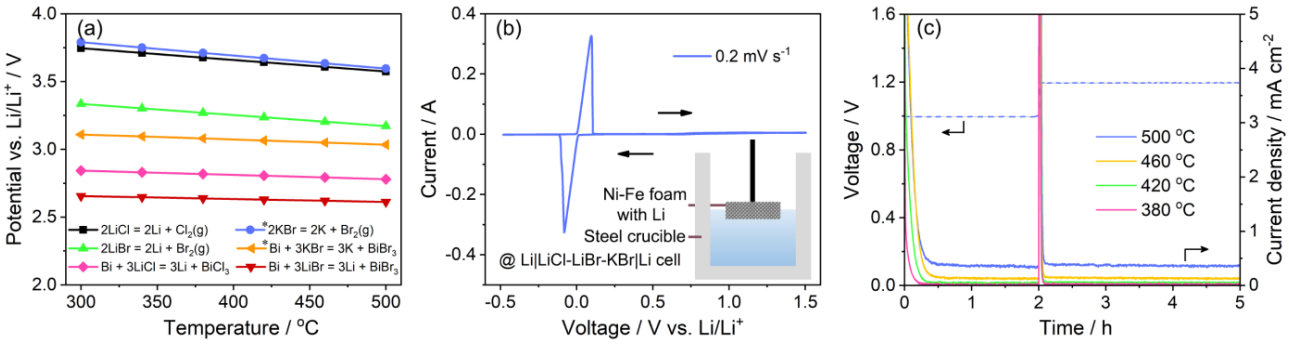

Figure 5. (a) Electrolysis potentials of possible reactions from 300 to 500 ^{o}C. (b) CV curve of Li|LiCl-LiBr-KBr|Li symmetrical cell. (c) Stepped potential measurement of Li|LiCl-LiBr-KBr|Bi cell from 500 to 380 ^{o}C. Note: potentials for reactions (*) in (a) are amended to Li/Li^{+}.

The solution of lithium in the electrolyte could cause self-discharge and so result in low Coulombic efficiency. We employed the stepped-potential method with constant voltage charging at 1 V for 2 h and then 1.2 V for 3 h to evaluate the self-discharge phenomenon at different temperatures. As shown in Figure 5c, the self-discharge currents are all less than 0.5 mA cm^{-2} from 500 to 380 ^{o}C, suggesting the low solubility of lithium in LiCl-LiBr-KBr

electrolyte. Especially at 420 and 380 ºC, only 0.05 and 0.02 mA cm^{-2} of the self-discharge currents can be observed, respectively, which is highly comparable and even lower than previous reported work [22]. The suppressed self-discharge behavior at low work temperature confers a higher Coulombic efficiency on the battery during operation, consistent with the results shown in Figure 2f.

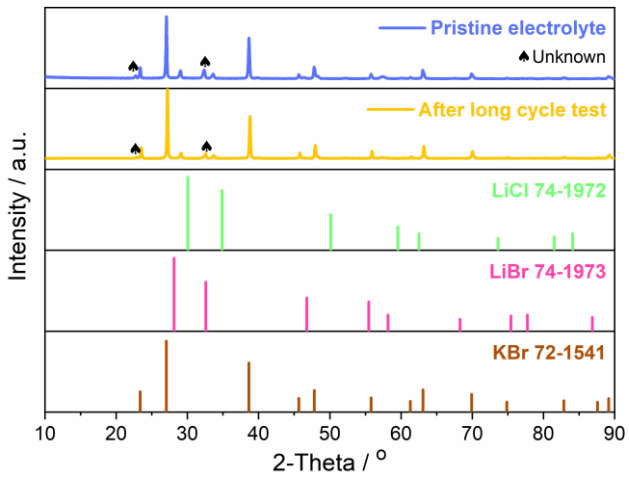

Figure 6. XRD patterns of LiCl-LiBr-KBr molten salt electrolyte before and after a long cycle test.

To verify the stability of the LiCl-LiBr-KBr molten salt, phase identification was performed on the electrolyte powder when the battery was cooled down to room temperature after a long cycle test (Figure 6). For comparison, the pristine LiCl-LiBr-KBr salt powder after pretreatment was also analyzed by XRD measurement. It should be noted that LiCl and LiBr exist in a solid solution form when the electrolyte is cooled from melting state to room temperature based on the LiCl-LiBr binary phase diagram (Figure S12). According to Vegard's law [36], the diffraction peaks of the solid solution should locate at between that of the constituents, depending on the mole composition. As shown in Figure 6, the diffraction peaks assignable to KBr and LiCl-LiBr solid solution can be observed in the pristine sample, indicating that the desirable electrolyte composition is obtained, and no side reactions occur during the pretreatment of the electrolyte. More importantly, there is no difference in the XRD

patterns of the electrolyte before and after the long cycle test, demonstrating the great stability of the LiCl-LiBr-KBr electrolyte in long-term operation. To be noticed, two unexpected peaks appear at 22.72 ^{o} and 32.35 ^{o}, which is interpretable that the electrolyte absorbs water or oxygen during the test sample preparation for XRD examination (Figure S13).

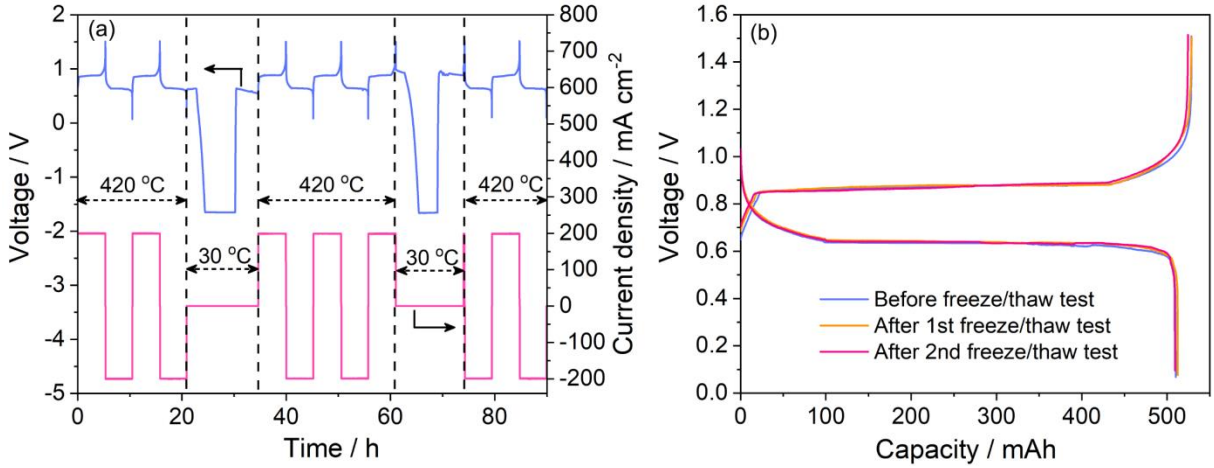

Figure 7. Freezing and thawing measurement (a) and the related voltage curves (b) of Li|LiCl-LiBr-KBr|Bi cell.

3.5. Freezing and Thawing Feature

Considering the characteristic of high-temperature operation, the LMB presents strong dependence on temperature control. If the thermal management system fails accidentally, the electrolyte will solidify and bring about volume change. The larger the electrolyte volume changes, the greater the mechanical damage to battery components, which may lead to deterioration of battery performance and even battery failure. Therefore, the freezing and thawing feature is very essential for LMBs. The electrochemical performance of Li|LiCl-LiBr-KBr|Bi cell against freezing/thawing attack was examined under both fully discharged and charged states (Figure 7a). It is worth noting that the Li|LiCl-LiBr-KBr|Bi cell exhibits superior recovery ability to regain the original condition in the subsequent cycles without open circuit or short circuit after freeze/thaw test. It shows similar voltage profiles without capacity and voltage loss before and after the freeze-thaw test (Figure 7b), suggesting the negligible

influence of volume change of LiCl-LiBr-KBr electrolyte on battery performance. These results demonstrate the excellent robustness of the Li|LiCl-LiBr-KBr|Bi cell against temperature fluctuation.

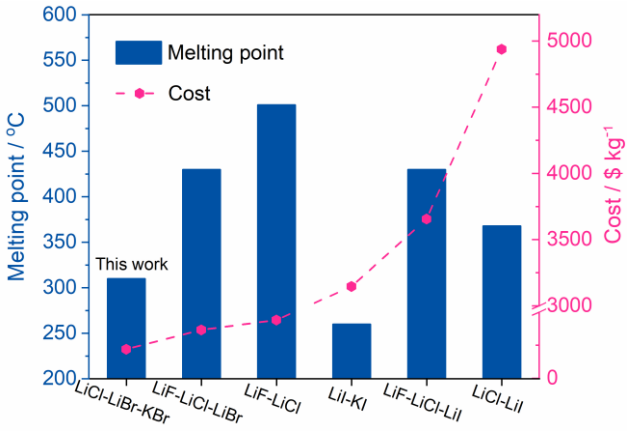

Figure 8. Melting point and cost of LiCl-LiBr-KBr electrolyte and some widely used Li-based electrolyte systems for liquid metal batteries.

3.6. Cost of LiCl-LiBr-KBr electrolyte

The competitiveness of the effective LiCl-LiBr-KBr electrolyte design lies in not only its superior electrochemical properties used for low-temperature LMBs, but also its desirable cost for commercial application potential. Based on the price of the raw materials (Table S3), the cost of LiCl-LiBr-KBr electrolyte is calculated to be 219.75 \$ kg^{-1}, which is significantly lower than that of other reported Li-based electrolytes (Table S4). The melting point and the cost of these electrolyte materials are plotted in Figure 8 for comparison. Remarkably, the elaborately designed LiCl-LiBr-KBr electrolyte presents an order of magnitude cost decrease with respect to the low-temperature LiI-based electrolyte systems. Even compared with the widely used LiF-LiCl-LiBr electrolyte, it still exhibits intriguing advantages, not only in its low melting point but also in the cost, which is only half of the LiF-LiCl-LiBr electrolyte. These attractive results make the LiCl-LiBr-KBr molten salt a promising electrolyte for low-temperature LMBs for commercial application.

4. Conclusion

In summary, a novel LiCl-LiBr-KBr ternary electrolyte is elaborately designed for LMBs based on the phase diagram and the isothermal conductivity calculations with the mass triangle model method. The designed electrolyte is aimed to circumvent the adverse effects of LMBs stemming from the high operating temperature. The LiCl-LiBr-KBr (33:29:38 mol%) electrolyte registers low melting point (327 ^{o}C), high ionic conductivity (1.573 S cm^{-1} at 420 ^{o}C), suitable density, and excellent chemical and electrochemical stabilities, which enables the LMB to offer superior electrochemical performance at low temperature of 420 ^{o}C. Specifically, the fabricated Li|LiCl-LiBr-KBr|Bi cell can efficiently work at 420 ^{o}C with high Coulombic efficiencies of greater than 97% at the current densities of 100-400 mA cm^{-2} and impressive energy efficiencies of 83.0% and 56% at 100 and 400 mA cm^{-2}, respectively, which outperforms most of the reported LMB system under the similar conditions. The constructed Li|LiCl-LiBr-KBr|Bi cell exhibits excellent rate performance with no capacity loss detectable when the charge/discharge current density increases from 100 to 400 mA cm^{-2}, and can cycle stably at 420 ^{o}C under 400 mA cm^{-2} over 170 charge and discharge cycles. Meanwhile, spectacular robustness can be achieved under large temperature fluctuation. These electrochemical performances are equivalent to that of the most potential high-temperature LMB systems, such as Li|LiF-LiCl-LiBr|Sb-Sn and Li|LiF-LiCl|Bi, while the operating temperature decreases substantially by 80-130 ^{o}C, but outperform the reported low-temperature systems, Li|LiCl-LiI|Bi-Pb and Li|LiI-KI|Bi-Sn. These encouraging results, together with the decent cost efficiency (219.75 \$ kg^{-1}), make the designed LiCl-LiBr-KBr salt a promising electrolyte for low-temperature LMBs.

This work provides an innovative strategy for Li-based LMBs to resolve the dilemma of high-temperature corrosion and low-temperature electrochemical performance deterioration. The findings will promote the commercial application of highly efficient and long-term stable LMB in large-scale energy storage.

CRediT authorship contribution statement

Hongliang Xie: Conceptualization, Methodology, Investigation, Data curation, Writing-original draft, Visualization. **Zhiyuan Chen:** Methodology, Data curation, Formal Analysis, Software. **Peng Chu:** Investigation, Formal Analysis, Data Curation. **Jie Wang:** Investigation, Formal Analysis. **Zehao Li:** Investigation, Data curation. **Hailei Zhao:** Conceptualization, Resources, Writing- review & editing, Supervision, Funding acquisition.

Declaration of competing interest

The authors declare that they have no known competing financial interests or personal relationships that could have appeared to influence the work reported in this paper.

Acknowledgments

This work was financially supported by National Key R&D Program of China (2018YFB0905600), National Natural Science Foundation of China (52074023 and 51634003), and Beijing Municipal Education Commission-Natural Science Foundation Joint Key Project (KZ201910005003).

Appendix A. Supplementary data

Supplementary data to this article can be found online.

References

[1] M. Pourbehzadi, T. Niknam, J. Aghaei, G. Mokryani, M. Shafie-khah, J.P.S. Catalão, Optimal operation of hybrid AC/DC microgrids under uncertainty of renewable energy resources: A comprehensive review, Int. J. Electr. Power Energy Syst. 109 (2019) 139–159. https://doi.org/10.1016/j.ijepes.2019.01.025.

[2] Y. Jin, K. Liu, J. Lang, D. Zhuo, Z. Huang, C. an Wang, H. Wu, Y. Cui, An intermediate temperature garnet-type solid electrolyte-based molten lithium battery for grid energy

storage, Nat. Energy. 3 (2018) 732–738. https://doi.org/10.1038/s41560-018-0198-9.

[3] O. Krishan, S. Suhag, An updated review of energy storage systems: Classification and applications in distributed generation power systems incorporating renewable energy resources, Int. J. Energy Res. 43 (2019) 6171–6210. https://doi.org/10.1002/er.4285.

[4] D. Larcher, J.M. Tarascon, Towards greener and more sustainable batteries for electrical energy storage, Nat. Chem. 7 (2015) 19–29. https://doi.org/10.1038/nchem.2085.

[5] H. Chamandoust, G. Derakhshan, S.M. Hakimi, S. Bahramara, Tri-objective scheduling of residential smart electrical distribution grids with optimal joint of responsive loads with renewable energy sources, J. Energy Storage. 27 (2020) 101112. https://doi.org/10.1016/j.est.2019.101112.

[6] A.R. Dehghani-Sanij, E. Tharumalingam, M.B. Dusseault, R. Fraser, Study of energy storage systems and environmental challenges of batteries, Renew. Sustain. Energy Rev. 104 (2019) 192–208. https://doi.org/10.1016/j.rser.2019.01.023.

[7] S. Chu, A. Majumdar, Opportunities and challenges for a sustainable energy future, Nature. 488 (2012) 294–303. https://doi.org/10.1038/nature11475.

[8] J. Lang, K. Liu, Y. Jin, Y. Long, L. Qi, H. Wu, Y. Cui, A molten battery consisting of Li metal anode, $AlCl_3$-LiCl cathode and solid electrolyte, Energy Storage Mater. 24 (2020) 412–416. https://doi.org/10.1016/j.ensm.2019.07.027.

[9] D.M. Davies, M.G. Verde, O. Mnyshenko, Y.R. Chen, R. Rajeev, Y.S. Meng, G. Elliott, Combined economic and technological evaluation of battery energy storage for grid applications, Nat. Energy. 4 (2019) 42–50. https://doi.org/10.1038/s41560-018-0290-1.

[10] H. Kim, D.A. Boysen, J.M. Newhouse, B.L. Spatocco, B. Chung, P.J. Burke, D.J. Bradwell, K. Jiang, A.A. Tomaszowska, K. Wang, W. Wei, L.A. Ortiz, S.A. Barriga, S.M. Poizeau, D.R. Sadoway, Liquid metal batteries: Past, Present, and Future, Chem. Rev. 113 (2013) 2075–2099. https://doi.org/10.1021/cr300205k.

[11] H. Li, H. Yin, K. Wang, S. Cheng, K. Jiang, D.R. Sadoway, Liquid Metal Electrodes for Energy Storage Batteries, Adv. Energy Mater. 6 (2016) 1600483. https://doi.org/10.1002/aenm.201600483.

[12] K. Cui, F. An, W. Zhao, P. Li, S. Li, C. Liu, X. Qu, Feasibility Research of SS304 Serving as the Positive Current Collector of Li||Sb-Sn Liquid Metal Batteries, J. Phys. Chem. C. 125 (2021) 237–245. https://doi.org/10.1021/acs.jpcc.0c09629.

[13] D.J. Bradwell, H. Kim, A.H.C. Sirk, D.R. Sadoway, Magnesium-antimony liquid metal battery for stationary energy storage, J. Am. Chem. Soc. 134 (2012) 1895–1897. https://doi.org/10.1021/ja209759s.

[14] K. Xu, Electrolytes and interphases in Li-ion batteries and beyond, Chem. Rev. 114 (2014) 11503–11618. https://doi.org/10.1021/cr500003w.

[15] L.Z. Fan, H. He, C.W. Nan, Tailoring inorganic–polymer composites for the mass production of solid-state batteries, Nat. Rev. Mater. 6 (2021) 1003–1019. https://doi.org/10.1038/s41578-021-00320-0.

[16] W. Zhao, P. Li, Z. Liu, D. He, K. Han, H. Zhao, X. Qu, High-Performance Antimony-Bismuth-Tin Positive Electrode for Liquid Metal Battery, Chem. Mater. 30 (2018) 8739–8746. https://doi.org/10.1021/acs.chemmater.8b01869.

[17] J. Xu, K. Liu, Y. Jin, B. Sun, Z. Zhang, Y. Chen, D. Su, G. Wang, H. Wu, Y. Cui, A Garnet-Type Solid-Electrolyte-Based Molten Lithium−Molybdenum−Iron(II) Chloride Battery with Advanced Reaction Mechanism, Adv. Mater. 32 (2020) 2000960. https://doi.org/10.1002/adma.202000960.

[18] H. Li, K. Wang, S. Cheng, K. Jiang, High Performance Liquid Metal Battery with Environmentally Friendly Antimony-Tin Positive Electrode, ACS Appl. Mater. Interfaces. 8 (2016) 12830–12835. https://doi.org/10.1021/acsami.6b02576.

[19] H. Li, K. Wang, H. Zhou, X. Guo, S. Cheng, K. Jiang, Tellurium-tin based electrodes

enabling liquid metal batteries for high specific energy storage applications, Energy Storage Mater. 14 (2018) 267–271. https://doi.org/10.1016/j.ensm.2018.04.017.

[20] H. Xie, H. Zhao, J. Wang, P. Chu, Z. Yang, C. Han, Y. Zhang, High-performance bismuth-gallium positive electrode for liquid metal battery, J. Power Sources. 472 (2020) 228634. https://doi.org/10.1016/j.jpowsour.2020.228634.

[21] X. Ning, S. Phadke, B. Chung, H. Yin, P. Burke, D.R. Sadoway, Self-healing Li-Bi liquid metal battery for grid-scale energy storage, J. Power Sources. 275 (2015) 370–376. https://doi.org/10.1016/j.jpowsour.2014.10.173.

[22] J. Kim, D. Shin, Y. Jung, S.M. Hwang, T. Song, Y. Kim, U. Paik, LiCl-LiI molten salt electrolyte with bismuth-lead positive electrode for liquid metal battery, J. Power Sources. 377 (2018) 87–92. https://doi.org/10.1016/j.jpowsour.2017.11.081.

[23] H. Yu, H. Lu, X. Hu, J. Liu, Y. Cao, LiI-KI and LAGP electrolytes with a bismuth-tin positive electrode for the development of a liquid lithium battery, Mater. Chem. Phys. 247 (2020) 122865. https://doi.org/10.1016/j.matchemphys.2020.122865.

[24] P. Masset, R.A. Guidotti, Thermal activated (thermal) battery technology. Part II. Molten salt electrolytes, J. Power Sources. 164 (2007) 397–414. https://doi.org/10.1016/j.jpowsour.2006.10.080.

[25] L. Redey, Overcharge Protection in Li-Alloy/Metal Disulfide Cells, ECS Proc. Vol. 1987–7 (1987) 631–636. https://doi.org/10.1149/198707.0631pv.

[26] T. D. Kaun, Li-AI/FeS Cell with LiCI-LiBr-KBr Electrolyte, (1985).

[27] T.D. Kaun, Modification of LiCl-LiBr-KBr Electrolyte for LiAl/FeS_2 Batteries, ECS Proc. Vol. 1996–7 (1996) 342–354. https://doi.org/10.1149/199607.0342pv.

[28] T.D. Kaun, Evaluation of LiCl-LiBr-KBr Electrolyte forLi-Alloy/Metal Disulfide Cells, ECS Proc. Vol. 1987–7 (1987) 621–630. https://doi.org/10.1149/198707.0621pv.

[29] H. Kim, D.A. Boysen, T. Ouchi, D.R. Sadoway, Calcium-bismuth electrodes for large-

scale energy storage (liquid metal batteries), J. Power Sources. 241 (2013) 239–248. https://doi.org/10.1016/j.jpowsour.2013.04.052.

[30] Z.G. Yu, H.Y. Leng, L.J. Wang, K.C. Chou, Computational study on various properties of CaO-Al_2O_3-SiO_2 mold flux, Ceram. Int. 45 (2019) 7180–7187. https://doi.org/10.1016/j.ceramint.2018.12.225.

[31] G.J. Janz, Thermodynamic and transport properties for molten salts: correlation equations for critically evaluated density, Surface Tension, Electrical Conductance, and Viscosity Data, J. Phys. Chem. Ref. Data. 17 (1988) 1–309.

[32] W. Weppner, R.A. Huggins, Thermodynamic Properties of the Intermetallic Systems Lithium-Antimony and Lithium-Bismuth, J. Electrochem. Soc. 125 (1978) 7–14. https://doi.org/10.1149/1.2131401.

[33] K. Wang, K. Jiang, B. Chung, T. Ouchi, P.J. Burke, D.A. Boysen, D.J. Bradwell, H. Kim, U. Muecke, D.R. Sadoway, Lithium-antimony-lead liquid metal battery for grid-level energy storage, Nature. 514 (2014) 348–350. https://doi.org/10.1038/nature13700.

[34] T. Dai, Y. Zhao, X.H. Ning, R. Lakshmi Narayan, J. Li, Z. Shan, Capacity extended bismuth-antimony cathode for high-performance liquid metal battery, J. Power Sources. 381 (2018) 38–45. https://doi.org/10.1016/j.jpowsour.2018.01.048.

[35] J.S. Yeo, J.H. Lee, E.J. Yoo, Electrochemical properties of environment-friendly lithium-tin liquid metal battery, Electrochim. Acta. 290 (2018) 228–235. https://doi.org/10.1016/j.electacta.2018.09.072.

[36] A. Pritam, V. Shrivastava, Deviations from Vegard's Law and Intense Raman Scattering in Low-Doped $Bi_2Mo_{1-x}W_xO_6$ (x = 0–10%) Ceramics, Phys. Status Solidi Basic Res. 257 (2020) 1900450. https://doi.org/10.1002/pssb.201900450.